Int. J. Heat Mass Transfer. Vol. 31, No. 11, pp. 2347–2355, 1988
Printed in Great Britain

0017-9310/88 \$3.00+0.00

A new correlation for laminar mixed convection over a rotating sphere

GEORGES LE PALEC

Groupe de Recherche en Génie Thermique, Institut Universitaire de Technologie, Rue Engel Gros, 90016 Belfort Cédex, France

(*Received* 15 *September* 1987 *and in final form* 22 *March* 1988)

Abstract—In this paper, a theoretical analysis of laminar mixed convection around a rotating sphere in a stream is presented. The results show the effects of the viscous dissipation in the boundary layer. A new correlation for the average Nusselt (Sherwood) number is presented for a Prandtl (Schmidt) number ranging from 0.7 to 2730 and negligible dissipative effects. This correlation is validated with numerical and experimental results. It can be used for the entire mixed convection regime, under buoyancy assisting flow and uniform wall temperature conditions.

1. INTRODUCTION

IN THE field of published results about heat and mass transfer over axisymmetric bodies, the special case of the sphere has received much attention. Several simple correlations and experimental data for the average Nusselt number for both laminar free and forced convection around a non-rotating sphere have been presented [1, 2]. The average Sherwood number for a rotating sphere placed in a uniform stream with its axis of rotation parallel to the free stream velocity was measured by Furuta *et al.* [3]. This type of flow was also theoretically studied by Lee *et al.* [4].

The linkage of the three flows (i.e. free convection, forced stream and rotation) has been investigated more recently [5, 6]. The laminar three-dimensional boundary layer over a rotating sphere in forced flow with an arbitrary angle β_i between the direction of the stream and the axis of rotation was theoretically studied by using a Görtler type of series [7, 8]. It was found that the average Nusselt number slowly increases with increasing β_i, but this change is too low to be experimentally validated. The theoretical results were also compared with electrochemical measures for the axial flow case (i.e. $\beta_i = 0$) and the agreement between theory and data was satisfactory [9, 10].

A survey of the literature shows that no useful correlation for the average heat (mass) transfer coefficient has been proposed for the mixed convection regime under axial flow conditions. This is the purpose of this paper in which the viscous dissipation effects on mixed convection are also studied in order to point out the limitations of the correlation. From comparison with the previous published results [5, 7–10], equations and results referring to the correlation coefficients are new.

2. THEORETICAL ANALYSIS

Consideration is given to steady, laminar, dissipative, constant properties (except the density changes) and incompressible boundary-layer flow around a sphere which is maintained at uniform surface temperature T_w. This sphere rotates in a uniform flow with oncoming free stream velocity U_∞ and temperature T_∞. The axis of rotation is parallel to the direction of the stream which moves upward while gravity g_a acts in the opposite direction. A non-rotating orthogonal curvilinear coordinate system x, y, θ is chosen, as shown in Fig. 1. Let V_x, V_y, V_θ be the corresponding velocity components. The boundary-layer equations can be written as

$$\frac{\partial V_x}{\partial x}+\frac{\partial V_y}{\partial y}+\frac{V_x}{r}\frac{\mathrm{d}r}{\mathrm{d}x}=0 \quad (1)$$

$$V_x\frac{\partial V_x}{\partial x}+V_y\frac{\partial V_x}{\partial y}-\frac{V_\theta^2}{r}\frac{\mathrm{d}r}{\mathrm{d}x} = U\frac{\mathrm{d}U}{\mathrm{d}x}+\nu\frac{\partial^2 V_x}{\partial y^2}\pm g_a\beta_t(T-T_\infty)\sin\varepsilon \quad (2)$$

$$V_x\frac{\partial V_\theta}{\partial x}+V_y\frac{\partial V_\theta}{\partial y}+\frac{V_xV_\theta}{r}\frac{\mathrm{d}r}{\mathrm{d}x}=\nu\frac{\partial^2 V_\theta}{\partial y^2} \quad (3)$$

$$V_x\frac{\partial T}{\partial x}+V_y\frac{\partial T}{\partial y}=\alpha\frac{\partial^2 T}{\partial y^2}+\frac{\nu}{C_p}\left[\left(\frac{\partial V_x}{\partial y}\right)^2+\left(\frac{\partial V_\theta}{\partial y}\right)^2\right]. \quad (4)$$

The boundary conditions are

$$y=0;\quad T=T_w,\quad V_x=V_y=0,\quad V_\theta=r\omega$$
$$y\to\infty;\quad T\to T_\infty,\quad V_\theta\to 0,\quad V_x\to U. \quad (5)$$

In the foregoing equations, ω is the angular velocity of the sphere whereas U is the local free stream velocity which can be expressed from the potential-flow theory as [11]

$$U=\frac{3}{2}U_\infty\sin\frac{x}{L} \quad (6)$$

where L is the radius of the sphere. The radial distance from a surface point to the axis of rotation is

NOMENCLATURE

B — rotation parameter defined by equation $(8)_1$
C_p — specific heat at constant pressure [$\mathrm{J\,kg^{-1}\,K^{-1}}$]
E_c — Eckert number, $U_\infty^2/C_p(T_w - T_\infty)$
$f(\varepsilon,\eta), g(\varepsilon,\eta)$ — reduced stream functions defined in Table 1
g_a — gravitational acceleration [$\mathrm{m\,s^{-2}}$]
Gr — Grashof number defined by equation $(9)_1$
L — radius of the sphere [m]
Nu — local Nusselt number
$\overline{Nu}$ — average Nusselt number for mixed convection
$\overline{Nu}_f$ — average Nusselt number for pure forced convection
$\overline{Nu}_n$ — average Nusselt number for pure free convection
$\overline{Nu}_r$ — average Nusselt number for pure rotation
Pr — Prandtl number
r — radial distance from the axis of rotation [m]
Re_∞, Re_ω — Reynolds numbers defined by equations (9)
Sc — Schmidt number
$\overline{Sh}$ — average Sherwood number for mixed convection
$\overline{Sh}_f$ — average Sherwood number for pure forced convection
$\overline{Sh}_n$ — average Sherwood number for pure free convection
$\overline{Sh}_r$ — average Sherwood number for pure rotation
T — fluid temperature [K]
U — local free velocity [$\mathrm{m\,s^{-1}}$]
V_x, V_y, V_θ — velocity components for the x-, y- and θ-directions [$\mathrm{m\,s^{-1}}$]
x, y, θ — coordinates shown in Fig. 1 [m].

Greek symbols
α — thermal diffusivity of the fluid [$\mathrm{m^2\,s^{-1}}$]
β_t — coefficient of thermal expansion [$\mathrm{K^{-1}}$]
ε, η — adimensional coordinates defined in Table 1
θ_T — reduced temperature defined in Table 1
ν — kinematic viscosity [$\mathrm{m^2\,s^{-1}}$]
ω — spin velocity of the sphere [$\mathrm{rad\,s^{-1}}$]
Ω — Richardson number defined by equation $(8)_2$.

Subscripts
w — condition at wall
∞ — free stream condition.

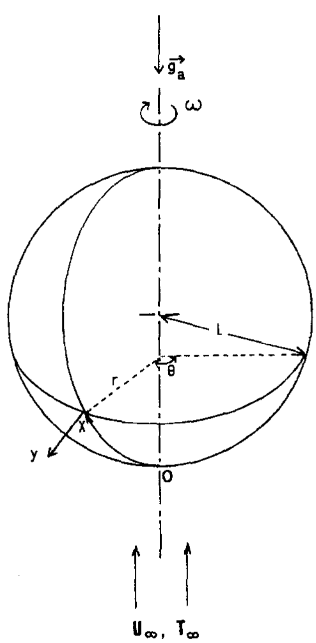

FIG. 1. The coordinates system.

$$r = L \sin\frac{x}{L}. \tag{7}$$

The other symbols in equations (1)–(4) are defined in the Nomenclature. For the entire mixed convection regime, three flow dominated cases can be defined from the values of the rotation parameter B and the Richardson number Ω [8]:

(1) the buoyancy force dominated case for $\Omega > 1$ and $B < \Omega$;

(2) the rotation dominated case for $B > 1$ and $B > \Omega$;

(3) the forced flow dominated case for $B < 1$ and $\Omega < 1$.

The definitions of B and Ω being, respectively

$$B = \frac{4}{9}\left(\frac{L\omega}{U_\infty}\right)^2 = \frac{4}{9}\left(\frac{Re_\omega}{Re_\infty}\right)^2, \quad \Omega = \frac{Gr}{Re_\infty^2} \tag{8}$$

with

$$Gr = \frac{g\beta_t(T_w - T_\infty)L^3}{\nu^2}, \quad Re_\infty = \frac{U_\infty L}{\nu}, \quad Re_\omega = \frac{\omega L^2}{\nu}. \tag{9}$$

Equations (1)–(5) are now transformed by introducing a (ε, η) dimensionless coordinate system, the reduced stream functions $f(\varepsilon,\eta)$ and $g(\varepsilon,\eta)$ and a dimensionless temperature $\theta_T(\varepsilon,\eta)$. The appropriate definitions of these parameters for each of the three above-cited cases are summarized in Table 1, where $\psi(x,y)$ and $\phi(x,y)$ are the stream functions which are

Table 1. Definitions of dimensionless coordinates, reduced stream functions and reduced temperature for the three flow dominated cases

	Buoyancy forces dominated case	Rotation dominated case	Forced flow dominated case
ε	x/L	x/L	x/L
η	$Gr^{1/4}\dfrac{y}{L}$	$\left[\dfrac{\omega R}{\nu\varepsilon}\right]^{1/2} y$	$\left[\dfrac{U}{L\nu\varepsilon}\right]^{1/2} y$
$f(\varepsilon,\eta)$	$\dfrac{\psi(x,y)}{\varepsilon\nu\, Gr^{1/4}}$	$\dfrac{\eta\psi(x,y)}{\omega r y}$	$\dfrac{\eta\psi(x,y)}{yU}$
$g(\varepsilon,\eta)$	$\dfrac{\phi(x,y)}{\varepsilon\nu\, Gr^{1/4}}$	$\dfrac{\eta\phi(x,y)}{\omega r y}$	$\dfrac{\eta\phi(x,y)}{\omega r y}$
$\theta_T(\varepsilon,\eta)$	$\dfrac{T-T_\infty}{T_w-T_\infty}$	$\dfrac{T-T_\infty}{T_w-T_\infty}$	$\dfrac{T-T_\infty}{T_w-T_\infty}$

related to the velocity components with the following equations:

$$V_x = \frac{1}{r}\frac{\partial\psi(x,y)r}{\partial y}$$

$$V_y = -\frac{1}{r}\frac{\partial\psi(x,y)r}{\partial x}$$

$$V_\theta = \frac{\partial\phi(x,y)}{\partial y}. \tag{10}$$

With these transformations, the continuity equation is identically satisfied. The momentum and energy equations become

$$f'''+K_1ff''-K_2f'^2+K_3g'^2+K_4\theta_T+K_5 = \varepsilon\left[f'\frac{\partial f'}{\partial\varepsilon}-f''\frac{\partial f}{\partial\varepsilon}\right] \tag{11}$$

$$g'''+K_1fg''-K_6f'g' = \varepsilon\left[f'\frac{\partial g'}{\partial\varepsilon}-g''\frac{\partial f}{\partial\varepsilon}\right] \tag{12}$$

$$Pr^{-1}\theta_T''+K_1f\theta_T'+K_7g'^2+K_8f'^2 = \varepsilon\left|f'\frac{\partial\theta_T}{\partial\varepsilon}-\theta_T'\frac{\partial f}{\partial\varepsilon}\right| \tag{13}$$

subjected to the boundary conditions

$$\begin{aligned} &\eta=0: \quad f=f'=g=0;\quad g'=K_9;\quad \theta_T=1\\ &\eta\to\infty: \quad f'\to K_{10};\quad g'\to 0;\quad \theta_T\to 0. \end{aligned} \tag{14}$$

The coefficients $K_1, K_2, \ldots, K_{10}$ are given in Table 2 and the primes denote differentiation with respect to η. Equations (11)–(14) are now transformed by assuming that the functions $f(\varepsilon,\eta)$, $g(\varepsilon,\eta)$ and $\theta_T(\varepsilon,\eta)$ have the following expansions:

$$\theta_T(\varepsilon,\eta) = \sum_{j=0}^{\infty}\theta_{T2j}(\eta)\varepsilon^{2j}$$

$$f(\varepsilon,\eta) = \sum_{j=0}^{\infty} f_{2j}(\eta)\varepsilon^{2j}$$

$$g(\varepsilon,\eta) = \sum_{j=0}^{\infty} g_{2j}(\eta)\varepsilon^{2j}. \tag{15}$$

Substituting equations (15) in equations (11)–(13) and boundary conditions (14) and collecting terms of different order in ε, as usual, a sequence of coupled ordinary differential equations is obtained [7]. From the definition of the Nusselt number

$$Nu = \frac{hL}{\lambda} \quad \text{with} \quad h = \frac{-\lambda\left(\dfrac{\partial T}{\partial y}\right)_{y=0}}{T_w-T_\infty}. \tag{16}$$

it can be shown that the local Nusselt number is expressed as ($N = 0, 2, 4, \ldots$):

(1) buoyancy forces dominated case

$$Nu = -Gr^{1/4}\sum_{N=0}^{\infty}\theta_{TN}'(0)\varepsilon^N; \tag{17}$$

(2) rotation dominated case

$$Nu = -\left(Re_\omega\frac{\sin\varepsilon}{\varepsilon}\right)^{1/2}\sum_{N=0}^{\infty}\theta_{TN}'(0)\varepsilon^N; \tag{18}$$

(3) forced flow dominated case

$$Nu = -\left(Re_\infty\frac{3\sin\varepsilon}{2\varepsilon}\right)^{1/2}\sum_{N=0}^{\infty}\theta_{TN}'(0)\varepsilon^N. \tag{19}$$

The average Nusselt number, $\overline{Nu}$, is obtained from the integral

$$\overline{Nu} = \frac{1}{S}\int_S Nu\,\mathrm{d}S \tag{20}$$

where S is the area of the sphere.

Table 2. Definitions of coefficients $K_1, K_2, \ldots, K_{10}$ which appear in equations (11)–(13) and boundary conditions (14)

	Buoyancy forces dominated case	Rotation dominated case	Forced flow dominated case
K_1	$1+\varepsilon\cot\varepsilon$	$0.5+1.5\varepsilon\cot\varepsilon$	$0.5+1.5\varepsilon\cot\varepsilon$
K_2	1	$\varepsilon\cot\varepsilon$	$\varepsilon\cot\varepsilon$
K_3	$\varepsilon\cot\varepsilon$	$\varepsilon\cot\varepsilon$	$B\varepsilon\cot\varepsilon$
K_4	$\dfrac{\sin\varepsilon}{\varepsilon}$	$\dfrac{Gr}{Re_\omega^2}\dfrac{\varepsilon}{\sin\varepsilon}$	$\dfrac{4}{9}\Omega\dfrac{\varepsilon}{\sin\varepsilon}$
K_5	$\dfrac{9}{4}\dfrac{\cos\varepsilon\sin\varepsilon}{\varepsilon}\Omega^{-1}$	$B^{-1}\varepsilon\cot\varepsilon$	0
K_6	$1+\varepsilon\cot\varepsilon$	$2\varepsilon\cot\varepsilon$	$2\varepsilon\cot\varepsilon$
K_7	$\Omega E_c\varepsilon^2 B$	$\dfrac{9}{4}E_c B\sin^2\varepsilon$	$\dfrac{9}{4}E_c B\sin^2\varepsilon$
K_8	$\Omega E_c\varepsilon^2$	$\dfrac{9}{4}E_c B\sin^2\varepsilon$	$\dfrac{9}{4}E_c\sin^2\varepsilon$
K_9	$1.5\dfrac{\sin\varepsilon}{\varepsilon}\sqrt{\left(\dfrac{B}{\Omega}\right)}$	1	1
K_{10}	$1.5\dfrac{\sin\varepsilon}{\varepsilon}\Omega^{-1/2}$	$B^{-1/2}$	1

3. NUMERICAL RESULTS

The set of coupled ordinary differential equations has been solved with the fourth-order Runge–Kutta–Gill procedure. Four terms of series (15) are sufficient to get a good accuracy. As it is seen from equations (11)–(13) and boundary conditions (14), the local Nusselt number is correlated to the following adimensional parameters:

(a) the rotation parameter B;
(b) the Richardson number Ω;
(c) the Eckert number E_c;
(d) the Prandtl number Pr.

Numerical calculations were performed for $0 \leqslant B \leqslant 100$, $0 \leqslant \Omega \leqslant 1000$, $0 \leqslant E_c \leqslant 0.01$ and $1 \leqslant Pr \leqslant 2730$.

In Fig. 2, the average Nusselt number $\overline{Nu}\,Re_\omega^{-1/2}$ is plotted against Ω for $Pr = 1$ and several values of B and E_c: the average heat transfer rate is seen to increase as the Richardson number increases for small values of the rotation parameter ($B = 1$) and negligible dissipative effects ($E_c = 0$). The increase of $\overline{Nu}\,Re_\omega^{-1/2}$ appears lower as the angular velocity is higher ($B = 10$) and it becomes negligible for $B = 100$, the centrifugal forces then being too high as compared with the buoyancy forces. As shown in the figure for $B = 1$ and 10 and $E_c = 0.005$ and 0.01, the viscous dissipation in the boundary layer produces smaller values of the average Nusselt number and dissipative effects increase with an increasing angular velocity. For $B = 100$, these effects become higher than the buoyancy force ones and the heat transfer rate is lower for mixed convection ($\Omega = 10$) than for the pure rotation case ($\Omega \to 0$). The shape and values of the profiles depend on the Prandtl number as shown in Figs. 3 and 4 where $\overline{Nu}\,Re_\omega^{-1/2}$ has been reported against Ω for $Pr = 10$ and 100, respectively. It is noted that an increase of the Prandtl number yields an increase in the viscous dissipation effects.

4. THE CORRELATION

For many heat-transfer applications, the viscous dissipation in the boundary layer is negligible so that E_c can be set equal to zero in the governing equations. A general correlation for the average Nusselt number has been developed with this assumption: the results that appear in Figs. 2–4 enable the limitations of such an equation to be seen for most practical cases ($Pr \leqslant 100$). For higher Prandtl numbers ($100 < Pr \leqslant 2730$), numerical calculations were performed for $0 \leqslant B \leqslant 25$ and $0 \leqslant \Omega \leqslant 100$ and the viscous dissipation was found negligible for $E_c < 0.0001$. As discussed before, the average Nusselt number $\overline{Nu}$ is correlated to the Prandtl number, the Richardson

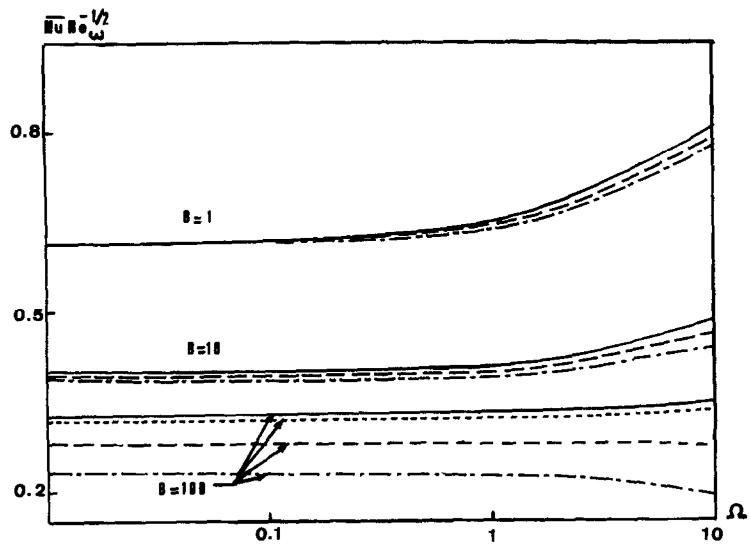

FIG. 2. Average Nusselt number vs Ω for $Pr = 1$: ——, $E_c = 0$; - - - -, $E_c = 0.001$; — — —, $E_c = 0.005$; —·—·—, $E_c = 0.01$.

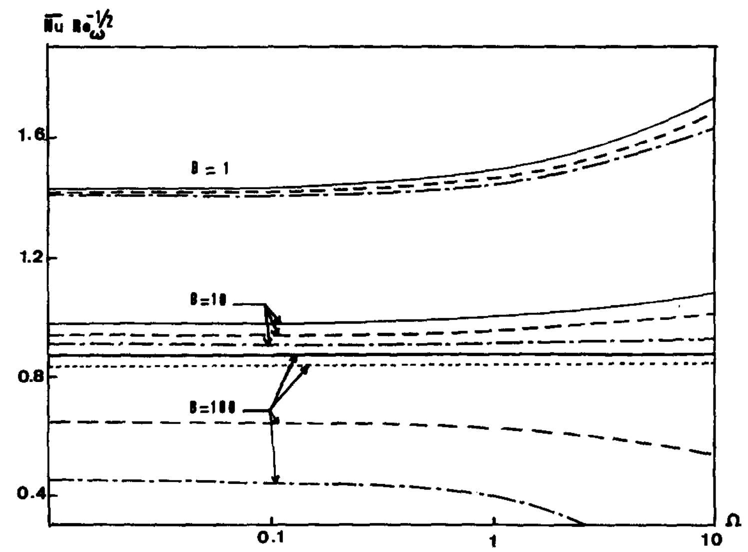

FIG. 3. Average Nusselt number vs Ω for $Pr = 10$: ——, $E_c = 0$; - - - -, $E_c = 0.001$; — — —, $E_c = 0.005$; —·—·—, $E_c = 0.01$.

number and the rotation parameter when $E_c = 0$. From definitions (8) and (9), it is seen that

$$\overline{Nu}\,Gr^{-1/4} = \overline{Nu}\,Re_\infty^{-1/2}\,\Omega^{-1/4} = \overline{Nu}\,Re_\omega^{-1/2}\left(\frac{9B}{4\Omega}\right)^{1/4}. \quad (21)$$

Following the analysis of Churchill and Usagi [12, 13], the average Nusselt number is assumed to be correlated to the average Nusselt number for pure free convection $\overline{Nu}_n$, the average Nusselt number for pure rotation $\overline{Nu}_r$ and the average Nusselt number for pure forced convection $\overline{Nu}_f$. One thus can write

$$\overline{Nu}^m = \overline{Nu}_n^m + \overline{Nu}_r^m + \overline{Nu}_f^m \quad (22)$$

where m is a constant exponent to be determined by comparing the correlation with the theoretically predicted results. Similarly, for mass transfer studies, the average Sherwood number equation is

$$\overline{Sh}^m = \overline{Sh}_n^m + \overline{Sh}_r^m + \overline{Sh}_f^m. \quad (23)$$

It should be noted that no theoretical basis allows one to write the average Nusselt (Sherwood) number as an average, because the differential equations system (11)–(13) is highly nonlinear. However, most of the correlating equations that have been proposed for other geometries have utilized the sum of some arbitrary power of correlating equations for the flow limited cases. Such equations appear to be generally satisfactory for mixed convection. The main differences between these correlations concern the value of the exponent m and the effect of the Prandtl number [13].

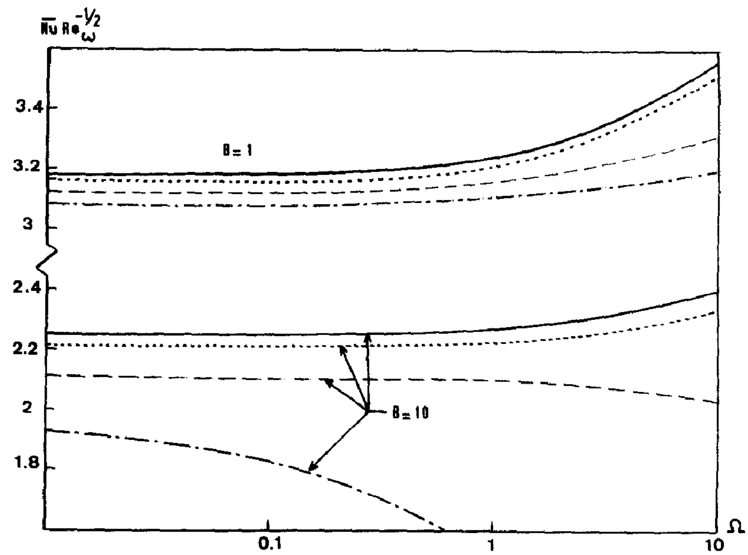

FIG. 4. Average Nusselt number vs Ω for $Pr = 100$: ——, $E_c = 0$; ----, $E_c = 0.001$; ——, $E_c = 0.005$; —·—·—, $E_c = 0.01$.

Numerical results which were obtained in the range $1 \leqslant Pr \leqslant 2730$ lead to the following relations:

for the pure free convection case ($\Omega \to \infty$, $B = 0$)

$$\overline{Nu}_n\, Gr^{-1/4} = 0.57 Pr^{1/4}(1-0.16 Pr^{-0.8}); \quad (24)$$

for the pure rotation case ($\Omega = 0$, $B \to \infty$)

$$\overline{Nu}_r\, Re_\omega^{-1/2} = 0.46 Pr^{1/3}(1-0.33 Pr^{-0.4}); \quad (25)$$

for the pure forced convection case ($\Omega = 0$, $B = 0$)

$$\overline{Nu}_f\, Re_\infty^{-1/2} = 0.81 Pr^{1/3}(1-0.09 Pr^{-0.5}). \quad (26)$$

The discrepancies between the theoretical and correlated values are listed in Table 3: one can see that the accuracy is good. The maximum deviation is 2.03% for $Pr = 10$ for the free convection case.

The limited cases, correlations (24)–(26) and equation (21), are now introduced in equation (22). One obtains

$$\overline{Nu} = 0.57(Pr\,Gr)^{1/4}(1-0.16 Pr^{-0.8}) \times [1+D(\Omega, B, Pr)]^{1/m} \quad (27)$$

where the function $D(\Omega, B, Pr)$ is defined as

$$D(\Omega, B, Pr) = A(Pr)\frac{Pr^{m/12}}{\Omega^{m/4}}[(0.988 A_1(Pr) B^{1/4})^m + (1.421 A_2(Pr))^m] \quad (28)$$

Table 3. Discrepancy (%) between predicted and correlated values for the flow limited cases

Pr	Pure free convection	Pure rotation	Pure forced convection
1	0.25	0.58	0.40
10	2.03	1.29	0.24
100	0.84	0.65	0.03
2730	0.002	1.40	0.35

with

$$A_1(Pr) = \frac{1-0.33 Pr^{-0.4}}{1-0.16 Pr^{-0.8}}$$

$$A_2(Pr) = \frac{1-0.09 Pr^{-0.5}}{1-0.16 Pr^{-0.8}}. \quad (29)$$

In equation (28), $A(Pr)$ is a correcting factor which takes into account the fact that fluids with lower Prandtl numbers have a higher sensitivity to buoyancy forces in comparison to fluids with higher Prandtl numbers.

5. RESULTS AND DISCUSSION

From the comparison of correlated and numerically predicted values, one has

$$m = 3$$

$$A(Pr) = 0.862 Pr^{-0.01}. \quad (30)$$

When no buoyancy forces occur, $A(Pr)$ should be taken as unity and Ω can easily be removed from equation (27) by introducing equations (21). It should be noted that the value of exponent m is the same as Armaly *et al.* found for the case of mixed convection over vertical, horizontal and inclined flat plates [14].

Figure 5 shows the ratio $(\overline{Nu}/\overline{Nu}_n)^3$ as a function of the rotation parameter B for $Pr = 1$ and 10 and for several Richardson numbers ($\Omega = 0.1, 1, 10, 100$). On Fig. 6 correlated values with a higher Prandtl number ($Pr = 100$ and 2730) have been reported. For all flow configurations, the results obtained from equation (27) and theory agree with each other. The maximum deviation (7%) is observed for $\Omega = 1$, $Pr = 2730$ and $B \leqslant 1$: the correlation then provides smaller values

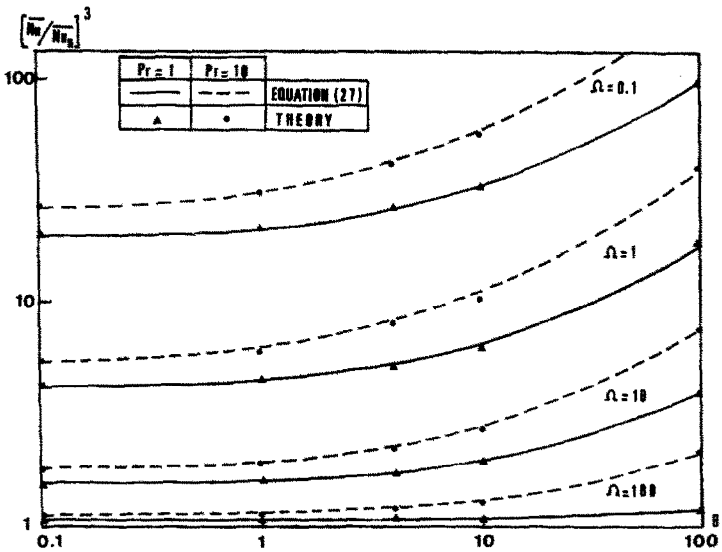

FIG. 5. Average Nusselt number for the mixed convection regime: comparison between correlated and numerical values, $Pr = 1$ and 10.

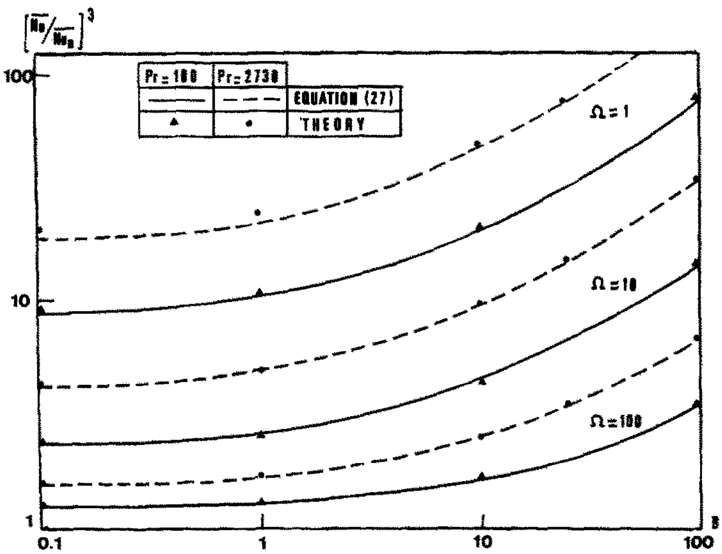

FIG. 6. Average Nusselt number for the mixed convection regime: comparison between correlated and numerical values, $Pr = 100$ and 2730.

than numerical calculations. For the rotation dominated case ($B \geqslant 10$), the discrepancy is less than 3% which is the same as for all other flow configurations.

As in refs. [2, 14], the upper and lower bounds of the mixed convection regime can be quantified by specifying a 5% departure from the three limited average Nusselt number cases. The resulting curves and flow configurations for $Pr = 1$ and 10 are shown in Fig. 7. The mixed convection regime is seen to occur for a wide range of buoyancy and rotation parameter values. Consequently, the pure forced convection, pure rotation and pure free convection regimes only exist under rather restrictive conditions.

Since the correlation has been validated, all the results can now be presented in a single figure the coordinates X and Y of which are

$$X = A(Pr)\left(\frac{9B}{4}\right)^{0.75}\left(\frac{\overline{Nu}_r\, Re_\omega^{-1/2}}{\overline{Nu}_n\, Gr^{-1/4}}\right)^3$$

$$Y = \Omega^{0.75}\left[\left(\frac{\overline{Nu}}{\overline{Nu}_n}\right)^3 - 1\right]. \qquad (31)$$

Figure 8 shows a logarithmic presentation of the curves which were obtained. From this figure and the knowledge of Pr, B and Ω, the average Nusselt number for the mixed convection regime can quickly be found by only using equation (24). For $Pr = 2730$, one also has reported some experimental data which were carried out from an electrochemical method [10]: the ratios X and Y then stand for

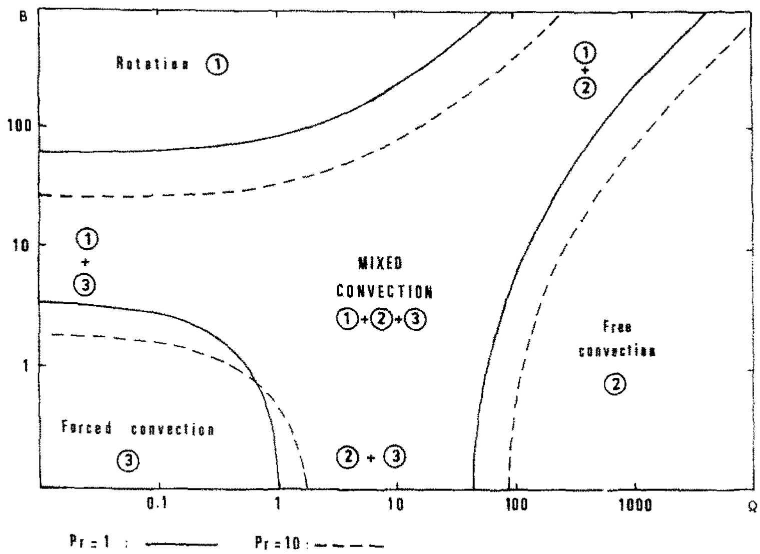

FIG. 7. The field of flow configurations with a B vs Ω logarithmic representation.

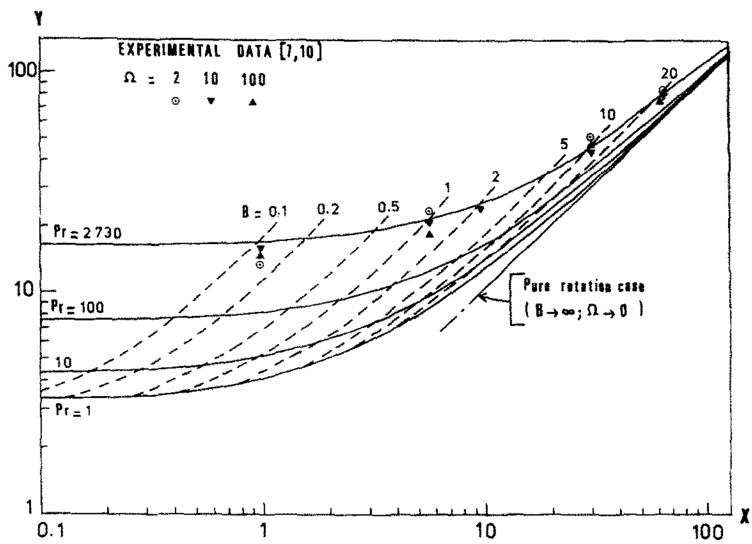

FIG. 8. Correlated results with X and Y coordinates and comparison of results with experimental data for $Sc = 2730$.

$$X = A(Sc)\left(\frac{9B}{4}\right)^{0.75}\left(\frac{\overline{Sh}_r\, Re_\omega^{-1/2}}{\overline{Sh}_n\, Gr^{-1/4}}\right)^3$$

$$Y = \Omega^{0.75}\left[\left(\frac{\overline{Sh}}{\overline{Sh}_n}\right)^3 - 1\right] \quad (32)$$

wherein Sc is the Schmidt number. The figure exhibits a reasonable agreement with the correlated values, especially for the rotation dominated case. For small values of the rotation parameter, the correlation deviates from experimental results. As explained in ref. [8], this discrepancy may be attributed both to the separation flow and the hypothesis of the potential-flow solution which was retained for theoretical calculations. It also should be noted that the linear assumption for the average Sherwood number (equation (23)) is a possible manifestation of this fact.

Before concluding this section, one must add that although the correlation is based upon numerical calculations in the range $1 \leqslant Pr \leqslant 2730$, equation (27) has been tested for the case of air ($Pr = 0.7$): the results show a 9% maximum departure from numerical results for $B = 100$ and $\Omega = 10$. The discrepancy is about 3% for $B = 10$ and 1% for $B = 1$. These results together with the previous results show that the proposed correlation may be applied in most of the practical cases embodied in laminar mixed convection.

6. CONCLUSION

A simple correlation for the average mixed convection Nusselt number for a rotating sphere placed in a uniform stream has been presented. This correlation has been tested for the entire mixed convection regime: it can be used under laminar buoyancy assisting flow and uniform wall temperature conditions for $0.7 \leqslant Pr \leqslant 2730$, all positive values of B and Ω and negligible viscous dissipation effects ($E_c = 0$). The results show a good agreement between the correlated and numerically predicted values. For non-negligible dissipative effects, Figs. 2–4 allow one to set the limitations of the formula.

REFERENCES

1. L. S. Klyachko, Heat transfer between a gas and a spherical surface with the combined action of free and forced convection, *J. Heat Transfer* **85C,** 355–357 (1963).
2. T. S. Chen and A. Mucoglu, Analysis of mixed forced and free convection about a sphere, *Int. J. Heat Mass Transfer* **20,** 867–875 (1977).
3. T. Furuta, T. Jimbo, M. Okasaki and R. Toei, Mass transfer to a rotating sphere in an axial stream, *J. Chem. Engng Japan* **8,** 456–462 (1975).
4. M. H. Lee, D. R. Jeng and K. J. De Witt, Laminar boundary layer transfer over rotating bodies in forced flow, *ASME J. Heat Transfer* **100,** 496–502 (1978).
5. G. Le Palec and M. Daguenet, Analysis of free convective effects about a rotating sphere in forced flow, *Int. Commun. Heat Mass Transfer* **11,** 409–416 (1984).
6. F. S. Lien, C. K. Chen and J. W. Cleaver, Mixed and free convection over a rotating sphere with blowing and suction, *ASME J. Heat Transfer* **108,** 398–404 (1986).
7. G. Le Palec, Etude de la convection mixte tridimensionnelle autour d'une sphère en rotation dans un écoulement ascendant de fluide newtonien, Thesis, Perpignan, France (1986).
8. G. Le Palec and M. Daguenet, Laminar three-dimensional mixed convection about a rotating sphere in a stream, *Int. J. Heat Mass Transfer* **30,** 1511–1523 (1987).
9. M. T. Razafiarimanana, Etude théorique et expérimentale de l'influence de la convection naturelle sur l'écoulement forcé engendré par une sphère en rotation plongée dans un écoulement vertical ascendant de fluide newtonien, Thesis, Perpignan, France (1986).
10. M. T. Razafiarimanana, M. Daguenet, G. Le Palec et F. Coeuret, Transfert de matière entre une sphère et un liquide newtonien en écoulement vertical ascendant, *Electrochim. Acta* **31,** 1103–1111 (1987).
11. H. Schlichting, *Boundary-layer Theory,* 6th Edn. McGraw-Hill, New York (1968).
12. S. W. Churchill and R. Usagi, A general expression for the correlation of rates of transfer and other phenomena, *A.I.Ch.E. Jl* **18,** 1121 (1972).
13. S. W. Churchill, A comprehensive correlating equation for laminar, assisting, forced and free convection, *A.I.Ch.E. Jl* **23,** 10–16 (1977).
14. B. F. Armaly, T. S. Chen and N. Ramachandran, Correlations for laminar mixed convection on vertical, inclined and horizontal flat plates with uniform surface heat flux, *Int. J. Heat Mass Transfer* **30,** 405–408 (1987).

CORRELATION NOUVELLE POUR LA CONVECTION MIXTE LAMINAIRE AUTOUR D'UNE SPHERE EN ROTATION

Résumé—On présente une analyse théorique de la convection mixte laminaire autour d'une sphère en rotation dans un écoulement forcé. Les résultats mettent en évidence l'influence de la dissipation visqueuse dans la couche limite. On propose aussi une corrélation donnant le nombre de Nusselt (Sherwood) moyen pour un nombre de Prandtl (Schmidt) compris entre 0,7 et 2730 et des effets dissipatifs négligeables. Cette relation est validée par les résultats numériques et expérimentaux. Elle peut être utilisée dans la totalité du domaine de convection mixte sous réserve que l'écoulement forcé ait la même direction que les forces de gravité et que la température de paroi soit constante.

EINE NEUE KORRELATION FÜR DIE LAMINARE MISCHKONVEKTION AN EINER ROTIERENDEN KUGEL

Zusammenfassung—Es wird eine theoretische Untersuchung der laminaren Mischkonvektion an einer angeströmten rotierenden Kugel vorgestellt. Die Ergebnisse zeigen den Einfluß der Reibungsverluste in der Grenzschicht. Es wird eine neue Korrelation für die mittlere Nusselt- (Sherwood-)Zahl vorgestellt für Prandtl- (Schmidt-)Zahlen im Bereich von 0,7 bis 2730 und vernachlässigbare Dissipation. Diese Beziehung wird mit numerischen und experimentellen Daten bestätigt. Sie kann für das gesamte Gebiet der Mischkonvektion angewandt werden bei auftriebsunterstützter Strömung und einheitlicher Wandtemperatur.

НОВОЕ СООТНОШЕНИЕ ДЛЯ СМЕШАННОЙ ЛАМИНАРНОЙ КОНВЕКЦИИ НАД ВРАЩАЮЩЕЙСЯ СФЕРОЙ

Аннотация—Представлен теоретический анализ ламинарной смешанной конвекции около сферн, вращающейся в потоке. Показано влияние вязкой диссипации в пограничном слое. Предложено новое критериальное соотношение для среднего числа Нуссельта (Шервуда) при числе Прандтля (Шмидта), изменяющемся от 0,7 до 2730 при пренебрежении эффектами диссипации. Это соотношение подтверждается численными и экспериментальными данными. Оно применимо для всего режима смешанной конвекции в условиях течения со спутной подъемной силой при постоянной температуре стенок.